ORIGINAL RESEARCH

α-synuclein interaction with zero-valent iron nanoparticles accelerates structural rearrangement into amyloid-susceptible structure with increased cytotoxic tendency

Seyedeh Sahar Tahaei Gilan[1,*]
Dorsa Yahya Rayat[1,*]
Twana Ahmed Mustafa[2]
Falah Mohammad Aziz[3]
Koorosh Shahpasand[4]
Keivan Akhtari[5]
Abbas Salihi[3,6]
Osama K Abou-Zied[7]
Mojtaba Falahati[8]

[1]Department of Cellular and Molecular Biology, Faculty of Advanced Science and Technology, Tehran Medical Sciences, Islamic Azad University, Tehran, Iran; [2]Department of Medical Laboratory Technology, Health Technical College, Erbil Polytechnic University, Erbil, Kurdistan Region, Iraq; [3]Department of Biology, College of Science, Salahaddin University-Erbil, Kurdistan Region, Iraq; [4]Department of Brain and Cognitive Sciences, Cell Science Research Center, Royan Institute for Stem Cell Biology and Technology, ACECR, Tehran, Iran; [5]Department of Physics, University of Kurdistan, Sanandaj, Iran; [6]Department of Medical Analysis, Faculty of Science, Tishk International University, Erbil, Iraq; [7]Department of Chemistry, Faculty of Science, Sultan Qaboos University, P.O. Box 36, Postal Code 123 Muscat, Oman; [8]Department of Nanotechnology, Faculty of Advanced Science and Technology, Tehran Medical Sciences, Islamic Azad University, Tehran, Iran

*These authors contributed equally to this work

Correspondence: Mojtaba Falahati
Department of Nanotechnology, Faculty of Advanced Science and Technology, Tehran Medical Sciences, Islamic Azad University, Tehran, Iran
Email mojtaba.falahati@alumni.ut.ac.ir

Osama K Abou-Zied
Department of Chemistry, Faculty of Science, Sultan Qaboos University, P.O. Box 36,123 Muscat, Oman
Email abouzied@squ.edu.om

Aim: It has been indicated that NPs may change the amyloidogenic steps of proteins and relevant cytotoxicity. Therefore, this report assigned to explore the impact of ZVFe NPs on the amyloidogenicity and cytotoxicity of α-synuclein as one of the many known amyloid proteins.

Methods: The characterization of α-synuclein at amyloidogenic condition either alone or with ZVFe NPs was carried out by fluorescence, CD, UV-visible spectroscopic methods, TEM study, docking, and molecular modeling. The cytotoxicity assay of α-synuclein amyloid in the absence and presence of ZVFe NPs was also done by MTT, LDH, and flow cytometry analysis.

Results: ThT fluorescence spectroscopy revealed that ZVFe NPs shorten the lag phase and accelerate the fibrillation rate of α-synuclein. Nile red and intrinsic fluorescence spectroscopy, CD, Congo red adsorption, and TEM studies indicated that ZVFe NP increased the propensity of α-synuclein into the amyloid fibrillation. Molecular docking study revealed that hydrophilic residues, such as Ser-9 and Lys-12 provide proper sites for hydrogen bonding and electrostatic interactions with adsorbed water molecules on ZVFe NPs, respectively. Molecular dynamics study determined that the interacted protein shifted from a natively discorded conformation toward a more packed structure. Cellular assay displayed that the cytotoxicity of α-synuclein amyloid against SH-SY5Y cells in the presence of ZVFe NPs is greater than the results obtained without ZVFe NPs.

Conclusion: In conclusion, the existence of ZVFe NPs promotes α-synuclein fibrillation at amyloidogenic conditions by forming a potential template for nucleation, the growth of α-synuclein fibrillation and induced cytotoxicity.

Keywords: α-synuclein, ZVFe NP, amyloid, cytotoxicity, spectroscopy

Introduction

Humans are widely exposed to nanoparticles (NPs) as they are ever-present in everyday life such as air pollutants[1], applicable materials in cosmetic by-products[2] and in nanomedicine.[3] Besides their purposeful role, their adverse effects on biochemical processes, such as cell integrity and protein conformational changes, remain unknown. Thus, investigating the interaction between biological systems and NPs, and the corresponding parameters influencing the cell viability and protein aggregation should be explored. The protein corona formation, as well as protein aggregation in the presence of NPs, may influence the NPs' fate in vivo.[4] Indeed,

NPs can heavily change the nucleation and aggregation phases of proteins.[5] The induction of several neurodegenerative disorders, such as Alzheimer, Parkinson's as well as Hungtinton's diseases is associated with the aggregation of proteins into amyloid forms.[6]

Nevertheless, there is no comprehensive detail to speculate evident activation or inhibition of the aggregation phases. For example, it was shown that the surface charges of the superparamagnetic iron-oxide NPs (SPION) could affect the fibrillation parameters of Aβ.[7] Surface charges, as well as the concentration of NPs, may play a dual effect on protein aggregation. While, lower doses of SPION can inhibit the Aβ aggregation, their higher doses accelerate the kinetic of Aβ amyloid induction.[7] In another study, it was revealed that the SPION having positive moieties could enhance protein aggregation at low NP doses in comparison with negatively charged SPIONs.[8] However, it was shown that polymeric NPs with different hydrophobic groups could inhibit the fibrillation of Aβ.[9] It was demonstrated that polymeric NPs delay essentially the nucleation and extension phases of Aβ fibrillation.[9]

Also, the interaction between NPs and proteins might influence the systemic cytotoxicity of NPs.[4] This induced cytotoxicity by NPs is heavily dependent on the inherent toxicity of NPs and the degree of protein aggregation around the NP surface.[10] Therefore, it is important to explore the effect of NPs on protein aggregation and induced cytotoxicity.

α-Synuclein shows a native disorder structure with 140 amino acid residues in the central nervous system with several bioactivities, such as microtubule-associated activity,[11] regulation of dopamine biosynthesis,[12] and neuronal plasticity.[13] It is believed, that conformational changes of the α-synuclein upon interaction with ligands like NPs may cause association of α-synuclein molecules into amyloid fibrils which is the major component of pathological disorder in neurodegenerative diseases.[14,15] However, the processes underlying the α-synuclein amyloid formation and its pathological effects in the presence of NPs are presently not well-explored.

Zero valent iron (ZVFe) NPs are widely used in environmental and water remediation,[16] antibacterial[17] and clinical systems[18] due to their unique properties and low toxicity. However, ZVFe NPs utilization can enhance the quantity of Fe ions to a great extent at a local dose in a short period of time. ZVFe NPs oxidation can also cause the generation of free radicals in biological systems which induce oxidative stress.[19] These outcomes can interrupt protein structures and cell membranes integrity and lead to protein aggregation and cell mortality.[20]

Also, an increase in Fe concentration and subsequent free radicals has been reported in the cortex and cerebellum of patients having neurodegenerative diseases like Alzheimer.[21]

Therefore, in the present study, the amyloid fibril formation and cytotoxicity of α-synuclein incubated with ZVFe NPs will be explored by different spectroscopic, theoretical and cellular methodologies.

Materials and methods
Materials
α-Synuclein, thioflavinT (ThT), nile red, Congo red, Dulbecco's minimum essential medium and Ham's F12 [DMEM: F12 (1:1)], fetal bovine serum (FBS), L-glutamine, penicillin, streptomycin, nerve growth factor (NGF) and 3-(4,5-dimethylthiazol-2-yl)-2,5-diphenyltetrazolium bromide (MTT) were purchased from Sigma (St. Louis, MO, USA). Lactate dehydrogenase (LDH) assay kit (Colorimetric) (ab102526) and Annexin V-FITC apoptosis staining/detection kit (ab14085) were purchased from Abcam Co. (Kendall Square, Suite B2304 Cambridge, MA 02139–1517 USA).

NP preparation
ZVFe NP was freshly dissolved in 1% (v/v) ethanol/water and was stored at room temperature until use. The concentration of ethanol did not exceed 1% in the prepared samples.

Fibrils formation
α-Synuclein solution (100 μM, with a molar absorptivity of 5960 cm^{-1} M^{-1} at 280 nm) was dissolved in 20 mM HEPES, 150 mM NaCl, pH 7.4 and agitated at 700 rev/min at 37 °C in the the presence of ZVFe NPs adapted from a previous study.[22] ZVFe NPs concentration was also set to 50 μg/mL.

ThT assay
Fibril formation was determined using ThT fluorescence by a Cary Eclipse VARIAN fluorescence spectrophotometer. The formation of α-synuclein fibrils incubated with ZVFe NPs (50 μg/mL) was investigated by detecting the fluorescence intensity of ThT in a diluted mixture of 2 μM protein and 15 μM ThT solution. Excitation and emission wavelengths were fixed at 440 and 485 nm,

respectively. The obtained results were fitted to a sigmoid curve according to the reported paper.[23]

Nile red fluorescence assay

α-Synuclein solution (100 μM) in the absence and presence of ZVFe NPs (50 μg/mL) were left for 45 h, then diluted to 2 μM in the presence of 15 μM nile red soloution. Samples were then excited at 530 nm and fluorescence intensssity was measured in the range of 610–740 nm.

Tyrosine fluorescence assay

α-Synuclein solution (100 μM) were incubated for 45 h with ZVFe NPs (50 μg/mL) and then diluted to 2 μM. α-Synuclein solutions were excited at 280 nm, and fluorescence intensssity was measured in the range of 290–370 nm.

Congo red binding assay

α-Synuclein solution (100 μM) incubated with ZVFe NPs (50 μg/mL) for 45 h were diluted to 5 μM and defined amount of Congo red was added to the samples. After 2 h of incubation at an ambient temperature in the dark, absorbance spectra were recorded in the range of 450–615 nm.

Far-UV circular dichroism (CD) measurement

α-Synuclein solution (100 μM) in the absence and presence of ZVFe NPs (50 μg/mL) were diluted to 3 μM and the CD spectra were determined after 45 h in the wavelengths of 190–260 nm, using an AVIV 215 spectropolarimeter (Aviv Associates, Lakewood, NJ, USA). The secondary structural changes of α-synuclein were then determined based on the change in ellipticity $[\theta]$. The change in $[\theta]$ was corrected for contribution from NPs and buffer solutions.

Transmission electron microcopy (TEM) study

Amyloid fibrils after 45 h, were dissolved in ethanol, sonicated and placed on copper grids at room temperature for 30 min. Electron micrographs of samples were then captured using a TEM EM10C – Zeiss (100 KV, Germany).

Simulation methods

A spherical cluster (1nm) and a slab (8 nm ×8 nm ×1.3 nm) were developed based on the Fe unit cell and used as a model for the ZVFe NPs in the simulations.[24] A docking investigation was carried out by using HEX 6.3 as the protein docking software which is equipped with spherical polar Fourier correlations.[25] Hex is defined as an interactive molecular graphics program for calculating protein-ligand interaction, presuming a ligand like NP is inflexible.[25] The slab models of ZVFe NPs were surrounded by 1000 water molecules at 298 K. Microcanonical (NVE) ensembles, the time step of 1 fs, and a total simulation time of 200 ps were used in the molding investigation. The molecular dynamics (MD) simulations were conducted using the Forcite code and Universal force field (UFF).[26]

Cell culture

SH-SY5Y cell line (obtained from Rouyn institute, Tehran, Iran) was used for cytotoxicity assay of ZVFe NPs, α-synuclein monomers, α-synuclein amyloid aged for 45 h, and ZVFe NPs/α-synuclein amyloid aged for 45 h. SH-SY5Y cells were cultured in DMEM: F12 (1:1) with 10% FBS, 2 mM L-glutamine, 1% penicillin, and 1% streptomycin and differentiated by NGF at 37 °C with 95% air and 5% CO_2.

MTT assay

The cellular viability treated with ZVFe NPs (10 μg/ml), α-synuclein (20 μM) monomers, α-synuclein amyloied (20 μM), and ZVFe NPs/α-synuclein amyloied (10 μg/ml/ 20 μM) were determined using MTT assay. The cells were exposed to the above-mentioned samples for 24 h. The treated cells with 20 mM HEPES, 150 mM NaCl, pH 7.4 were considered as control samples. The mitochondrial function was then investigated by 0.5 mg/mL MTT for 4 h, and the cell viability was quantified spectrophotometrically at 570 nm in Expert 96, Asys Hitch, Ec Austria.

LDH assay

LDH assay was done based on the manufacturer's protocol [(Colorimetric) (ab102526). The absorbance of formazan was then detected spectrophotometrically at 450 nm in ELISA reader (Expert 96, Asys Hitch, Ec Austria).

Flow cytometry analysis

Quantification of apoptosis using Annexin V/PI was done based on Apoptosis Staining/Detection Kit (ab14085). The stained cells were then collected and assayed by BD FACSCalibur (Becton Dickinson, San Jose, CA, USA).

Statistical analysis

The values obtained were shown as mean ± standard deviation (SD). Student's *t*-test was employed to explore and compare the data between the NPs-treated cells and the control samples, and the degree of significance was reported as *$P<0.05$; **$P<0.01$; ***$P<0.001$.

Results and discussion

ZVFe NP synthesis and characterization

ZVFe NPs were fabricated and fully characterized by different methods as reported in our recent work.[27] Briefly, it was displayed that the diameter, hydrodynamic radius and zeta potential values of ZVFe NPs were around 30 nm, 83.88 nm and −31.91±6.24 mV, respectively.[27]

NPs have been recently introduced to induce aggregation or disaggregation in protein molecules based on their chemical compositions, functional groups and concentrations. In this study, we explored the amyloidogenic impact of ZVFe NPs, man-made occurring NPs commonly present in the cosmetic products, water, and medicinal agents with no significant toxicity. To investigate if ZVFe NPs affect α-synuclein fibril formation, one concentration of this compound (50 μg/mL) added to the incubation medium. This concentration has been reported to be the maximum applied concentration of ZVFe NPs with minimum toxicity.[28] Also, for cellular assays, the concentration of ZVFe NP was diluted to 10 μg/mL which has been also revealed to have no cytotoxicity against cells.[28] The amyloid fibrillation phase was then studied by using several biophysical and cellular approaches.

ThT fluorescence assay

ThT fluorescence assay was prepared to determine the rate of α-synuclein fibril formation in the presence of ZVFe NPs. Kinetics of α-synuclein fibril formation either alone or with ZVFe NPs are depicted in Figure 1. It can be demonstrated a more significant increase of ThT fluorescence in α-synuclein with ZVFe NPs relative to α-synuclein alone over time. According to previous studies,[29,30] α-synuclein fibril formation showed a nucleated polymerization phase.

The ThT fluorescence kinetics analyses are reported in Table 1. It was seen that the K_{app} of α-synuclein fibrillation dramatically enhanced in the presence of ZVFe NPs (*$P<0.05$), whereas the lag time of α-synuclein fibrillation decreased to a certain extent (*$P<0.05$) (Table 1).

The results reveal that the presence of ZVFe NPs dramatically increased the α-synuclein fibril formation by
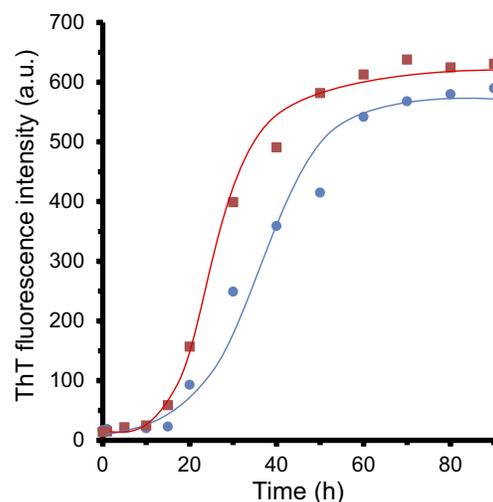

Figure 1 Kinetics of α-synuclein amyloid fibrillation as detected by ThT fluorescence assay. Protein samples (100 μM in the absence (circle) and presence of zero valent iron (ZVFe) NPs (square).

Table 1 Influence of zero valent iron (ZVFe) NPs on the kinetics parameters of α-synuclein fibrillation calculated by ThT fluorescence assay.*$P<0.05$ relative to the control group

	K_{app} (h^{-1})	Lag time (h)	Intensity (a.u.)
α-synuclein	0.071	16.91	631
α-synuclein/ZVFe NPs	0.060 (*$P<0.05$)	12.08 (*$P<0.05$)	590

decreasing the lag time and increasing the fibrillation rate constant which indicates that the ZVFe NPs provide a suitable environment to interact with prefibrillar molecules.

To assess the nile red fluorescence assay, tyrosine fluorescence assay, Congo red assay, and CD assay, the samples were read after 45 h of incubation (middle of the growth phase), with or without ZVFe NPs in the amyloidogenic condition. Also, the aliquots of amyloid samples after 45 h were used to assess the cytotoxicity effect of amyloid fibrils.

Nile red fluorescence assay

It has been well-documented that the structural changes of a protein like α-synuclein under amyloidogenic environment are assigned by the induction of hydrophobic patches on the protein structure.[31] For α-synuclein amyloid, a significant increase in nile red fluorescence intensity accompanied by a blue shift (from 673 to 656 nm) was observed when samples were incubated with ZVFe NPs (Figure 2). In fact,
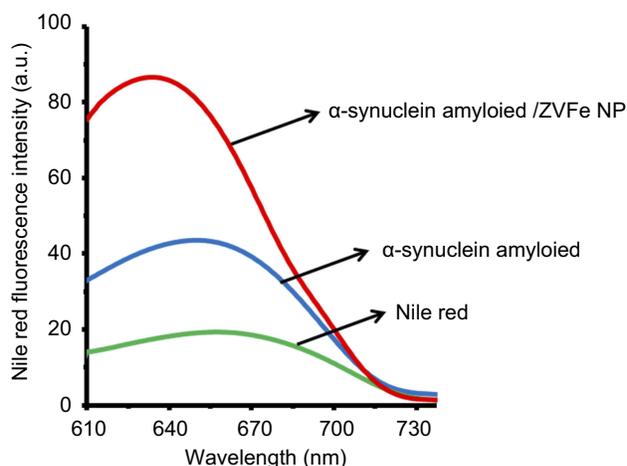
Figure 2 Effect of zero valent iron (ZVFe) NPs on surface hydrophobicity of α-synuclein as detected by nile red fluorescence assay after 45 h.

the increase in the fluorescence signal and the blue shift were more significant in the case of ZVFe NPs/α-synuclein amyloid, relative to those of α-synuclein amyloid alone. This data may reveal the ability of ZVFe NPs to accelerate the induction of hydrophobic patches in the structure of α-synuclein.

Tyrosine fluorescence assay

Tyrosine fluorescence assay was also performed to explore the microenvironmental changes around the tyrosine residues. As shown in Figure 3, a blue-shift (from 305 to 303 nm) with a decrease in intensity was detected for the tyrosine fluorescence in the presence of amyloid, indicating a structural alteration in the microenvironment of the tyrosine residues and a substantial alterations of the native structure of the protein. Also, the presence of ZVFe NPs in the amyloid sample resulted in a more pronounced blue shift (301 nm) and
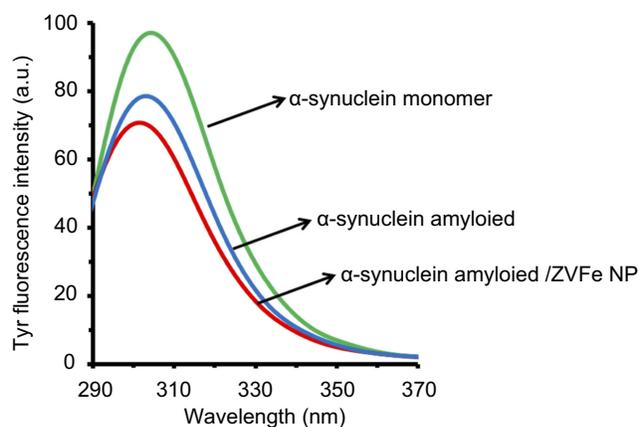
reduction in the fluorescence intensity of tyrosine (Figure 3) compared to free protein, suggesting that the NPs accelerate the α-synuclein structural alteration. The results indicate that the ZVFe NPs demonstrate their amyloidogenic effect by redirecting the α-synuclein aggregation pathway toward induction of amyloid fibrils with increased hydrophobic patches.

Congo red assay

As depicted in Figure 4, a significant increase in Congo red absorbance was observed with a red-shift (from 478 nm to 495 nm) upon incubation of α-synuclein in the amyloidogenic environment. Both absorbance and red-shift increase (from 478 nm to 502 nm) for α-synuclein with ZVFe NPs, indicating a strong interaction between Congo red and α-synuclein/ ZVFe NPs complex. This suggests the formation of α-synuclein amyloid fibrils is accelerated in the presence of ZVFe NPs.

CD study

To reveal whether structural alterations of α-synuclein induced by the amyloidogenic environment could be accelerated by ZVFe NPs, far-UV CD spectra were employed. As depicted in Figure 5, CD spectra of α-synuclein monomer and α-synuclein amyloid aged for 45 h show a predominantly random coil structure (minimum centered at 195 nm). However, in the presence of ZVFe NPs, a shift was observed in the structure of α-synuclein toward almost α-helix and β-sheet-rich structures (minimum appeared atf212 nm) in an amyloidogenic environment. Therefore, ZVFe NPs with applied concentration could accelerate amyloid formation determined by appearing a large minimum around 212 nm (Figure 5).
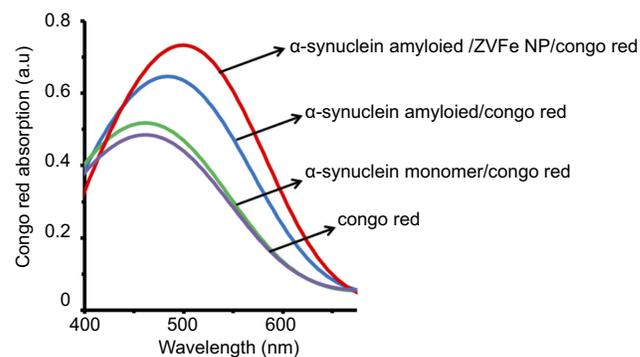

Figure 3 Effect of zero valent iron (ZVFe) NPs on conformational changes of α-synuclein as detected by tyrosine fluorescence assay after 45 h.

Figure 4 Congo red absorption spectra of α-synucle in monomer and amyloid with or without zero valent iron (ZVFe) NPs after 45 h.
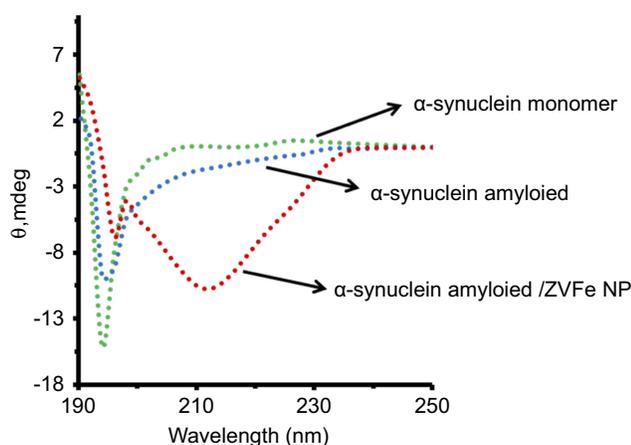
Figure 5 Effect of zero valent iron (ZVFe) NPs on the secondary structure of α-synuclein in the absence and presence of ZVFe NPs as detected by CD spectroscopy after 45 h.

TEM study

Figure 6 displays the TEM images of α-synuclein incubated for 45 h in an amyloidogenic buffer either alone or with ZVFe NPs. As represented in Figure 6A, in the native α-synuclein (no incubation time) as a control sample, no observable amyloid species were detected. However, after 45 h in an amyloidogenic condition, some oligomer forms of α-synuclein were observed (Figure 6B). In other side, in the presence of ZVFe NPs, some fibrils with common amyloid morphology were formed (Figure 6C). Indeed, we observed that the formation of a large number of amyloid fibrils were promoted in the presence of ZVFe NPs. This data further proves that ZVFe NPs activated the formation of fibrillary structures.

Molecular docking study

The interaction between NPs and protein plays a pivotal role in modulating protein structure and corresponding functions. Molecular docking represents an effective tool to study the interactions between molecules in complexes. Molecular docking also plays a crucial role in investigating protein

conformation and functions. In the current study, the NMR structure of human α-synuclein (PDB ID: 1XQ8) was used. Molecular docking was executed with the ZVFe cluster decorated by 12 water molecules as a model of hydrated ZVFe NPs.[24] The geometry of the hydrated cluster was optimized using UFF implemented in the Avogadro software (Libavogadro Library, Pittsburgh, PA, USA).[32] The calculated interaction energy was estimated to be −104.76 E-value. Visualization of the interacting residues was achieved by using CHIMERA (www.cgl.ucsf.edu/chimera) tool. The docked complex is depicted in Figure 7.

The ZVFe NPs with the nearest active site (4Å) is demonstrated in Figure 8. As can be seen, the hydrophilic residues Ser-9 and Lys-12 provide proper sites for hydrogen bonding and electrostatic interaction, respectively, with the adsorbed water molecules on ZVFe NPs.

Molecular dynamics study

MD simulation is an in silico modelling method for exploring conformational alteration of protein. The structure of α-synuclein with or without of ZVFe NP is displayed in Figure 9. It is clear that the interacted part of the protein is shifted from a natively disordered conformation toward a more packed structure. Indeed, as shown in Figure 9, in the beginning of running molecular modeling, the α-synuclein structure shows a random coil structure with very low helical content. However, after 200 PS and relevant interactions between ZVFe NP surface and α-synuclein, it was shown a tendency towards a higher α-helical conformation in the α-synuclein structure relative to the absence of interaction. This data indicated that interaction of ZVFe NPs with α-synuclein results in formation of more helical structure in protein structure. These findings are in good agreement with spectroscopy outcomes which showed that interaction of ZVFe NPs with α-synuclein led to structural changes of
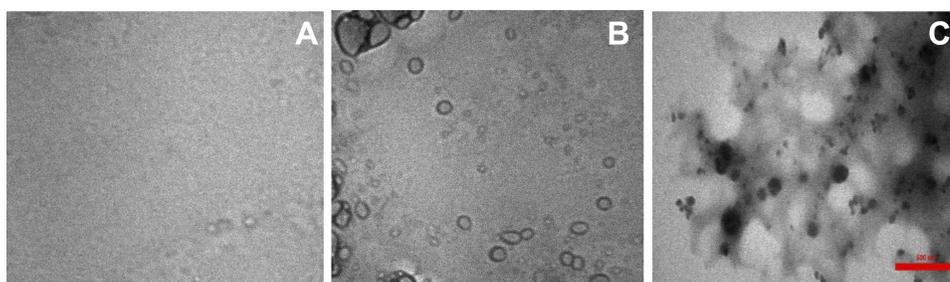

Figure 6 Transmission electron microscopy (TEM) images of α-synuclein incubated in the absence and presence of ZVFe NPs. (**A**) α-synuclein monomer, (**B**) α-synuclein amyloid, (**C**) α-synuclein amyloid/ZVFe NPs.
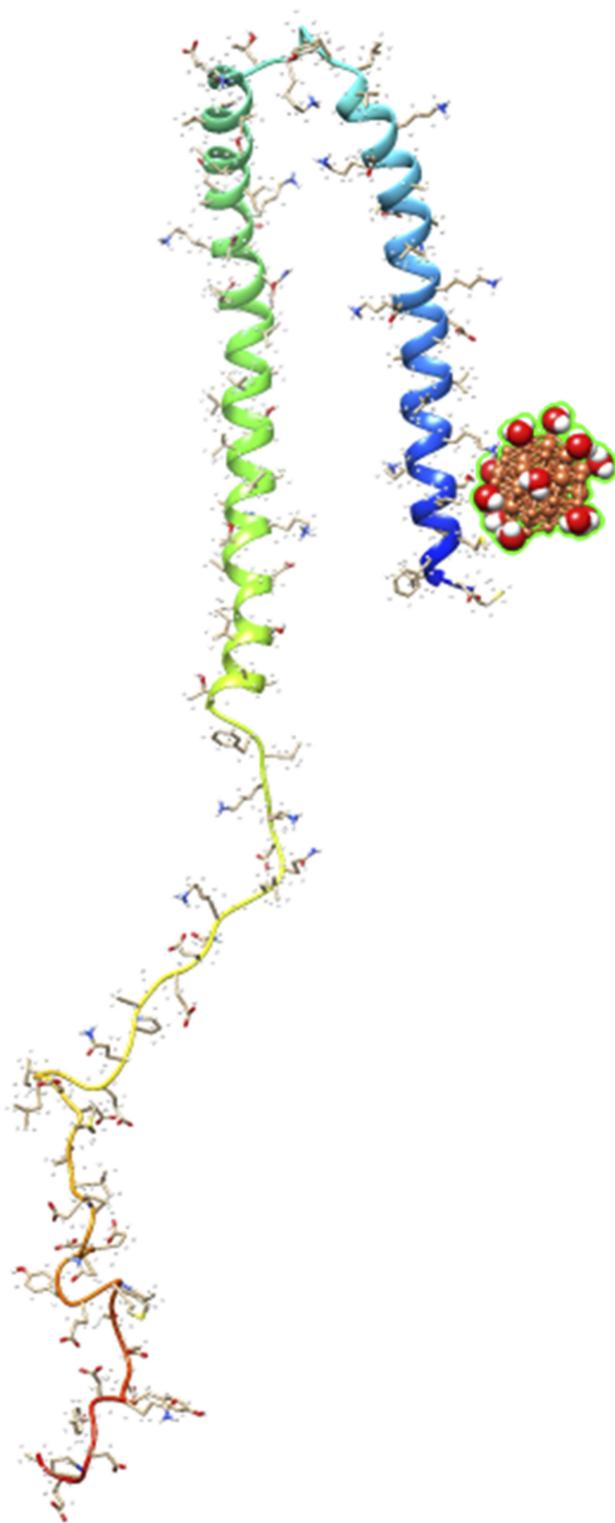
Figure 7 Molecular docking results are showing the binding mode of zero valent iron (ZVFe) NPs to α-synuclein. ZVFe NPs are depicted in ball model. Protein backbone of α-synuclein is demonstrated in the cartoon model.

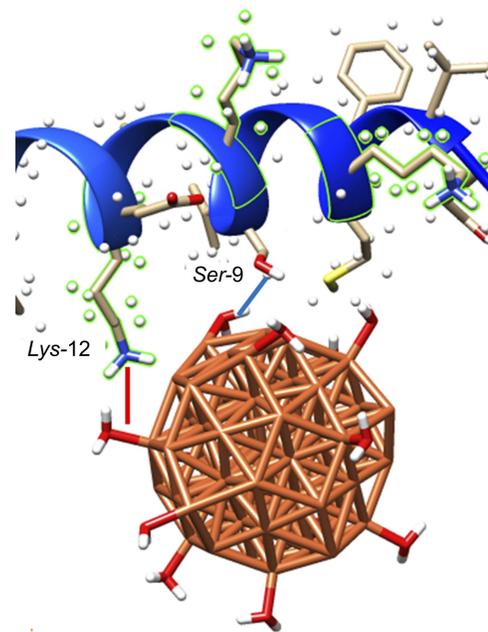α-synuclein toward a more hydrophobic and packed structure.

Figure 8 α-synuclein residues surrounding azero valent iron (ZVFe) NP are displayed. Hydrogen bond within 4 Å is shown as a blue line between the hydrated ZVFe NP and Ser-9, and electrostatic interaction within 4 Å is depicted as red line with Lys-12.

MTT assay

To assess the toxicity of amyloid species either alone or with ZVFe NPs, MTT assay was carried out. SH-SY5Y cells were incubated with ZVFe NPs, amyloid α-synuclein, and amyloid α-synuclein/ZVFe NPs for 24 h. While, no cytotoxicity was determined for negative control ZVFe NP (Figure 10) and α-synuclein monomer (data not shown), cell viability is markedly reduced after 24 h exposure to α-synuclein amyloid, and α-synuclein amyloid/ZVFe NPs (Figure 10). In other words, in the present of α-synuclein amyloid and α-synuclein amyloid/ZVFe NPs, the cell viability was reduced to 73% ±16.27 (*$P<0.05$) and 37% ±4.84 (**$P<0.01$), respectively. The enhancement in cytotoxicity was more pronounced ($^{###}P<0.01$) in α-synuclein amyloid/ZVFe NPs-treated cells than α-synuclein amyloid-treated cells. Therefore, in the presence of ZVFe NPs, α-synuclein amyloid is significantly more toxic compared to that in the absence of ZVFe NPs. As protein conformational changes and formation of the hydrophobic microenvironment in the course of during protein aggregation is a pivotal and usual characteristic of misfolded toxic samples.[23], we may propose that ZVFe NPs increases the formation of hydrophobic patches, as determined by spectroscopy assays, causing the formation of toxic aggregate samples.
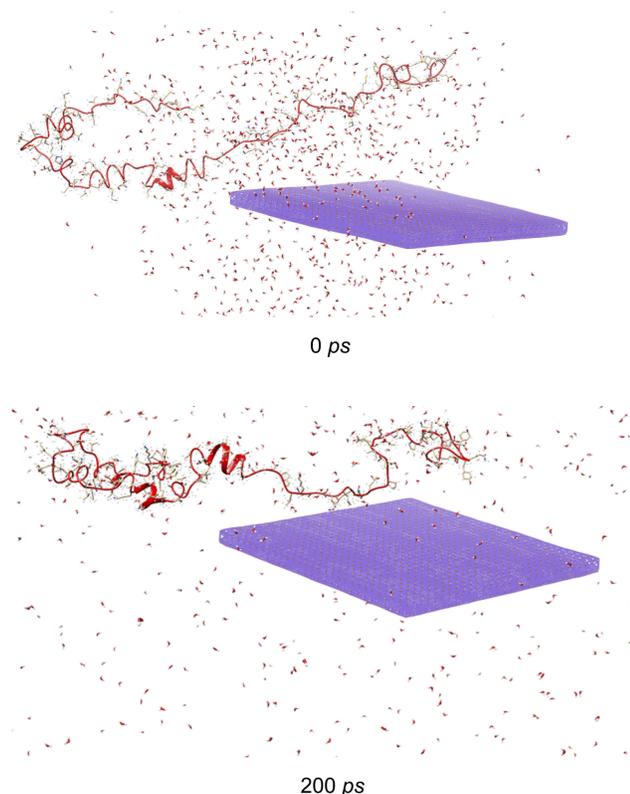
0 *ps*

200 *ps*

Figure 9 The structure of α-synuclein in the beginning (top) and after 200 ps evolution (bottom) with (zero valent iron) ZVFe NP. Interacted protein shifted from a natively disordered conformation toward a more packed arrangement.

LDH assay

LDH assay was done to explore the integrity of cell membrane in the presence of α-synuclein amyloid and α-synuclein amyloid/ZVFe NPs. α-Synuclein amyloid either alone or with ZVFe NPs aged for 45 h were diluted to the specified concentrations, and their related cytotoxicity against SH-SY5Y cells was evaluated by LDH assay. It was observed that ZVFe NPs (Figure 11) and α-synuclein monomer (data not shown) induced no significant LDH release in the SH-SY5Y cells compared to the negative control sample. Nevertheless, LDH releases significantly increased after 24 h exposure to α-synuclein amyloid and α-synuclein amyloid/ZVFe NPs to 131% ±17.62(*$P<0.05$) and 168% ±19.51(**$P<0.01$) (Figure 11), respectively. In fact, it was detected that the presence of ZVFe NPs induced more pronounced LDH release ([#]$P<0.05$) by α-synuclein amyloid in comparison with α-synuclein amyloid in the absence of ZVFe NP. Hence, it may be concluded that amyloid α-synuclein formation in the presence of ZVFe NPs is significantly accelerated and ZVFe NPs induced the formation of more toxic aggregated species in comparison with the results obtained without ZVFe NPs.
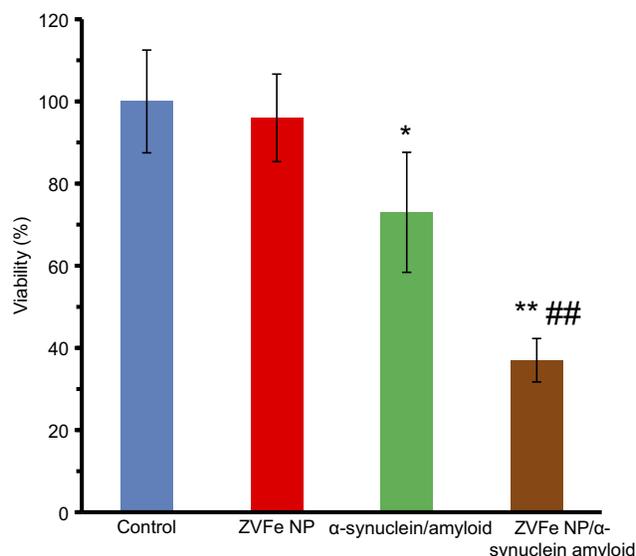

Figure 10 Cytotoxicity of α-synuclein aggregates formed with or without zero valent iron (ZVFe) NPs. *$P<0.05$ and **$P<0.01$, significantly different from control cells. [##]$P<0.01$, significantly different from cells exposed only to α-synuclein amyloid.
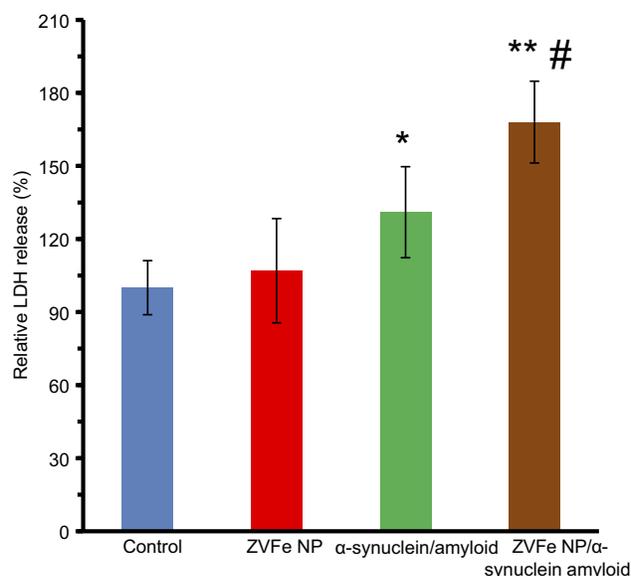

Figure 11 Lactate0 dehydrogenase (LDH) release of α-synuclein aggregates formed with or without ZVFe NPs. *$P<0.05$ and **$P<0.01$, significantly different from control cells. [#]$P<0.01$, significantly different from cells exposed only to α-synuclein amyloid.

Flow cytometry analysis

Flow cytometry assay was also performed in order to quantify the induction of apoptosis and necrosis in SH-SY5Y cells by α-synuclein amyloid and α-synuclein amyloid/ZVFe NPs samples. It was observed that 88.5% of cells are in viable cells quadrant (Q4) in the negative control samples (Figure 12A). Samples treated with α-synuclein monomer and ZVFe NPs showed almost the same results
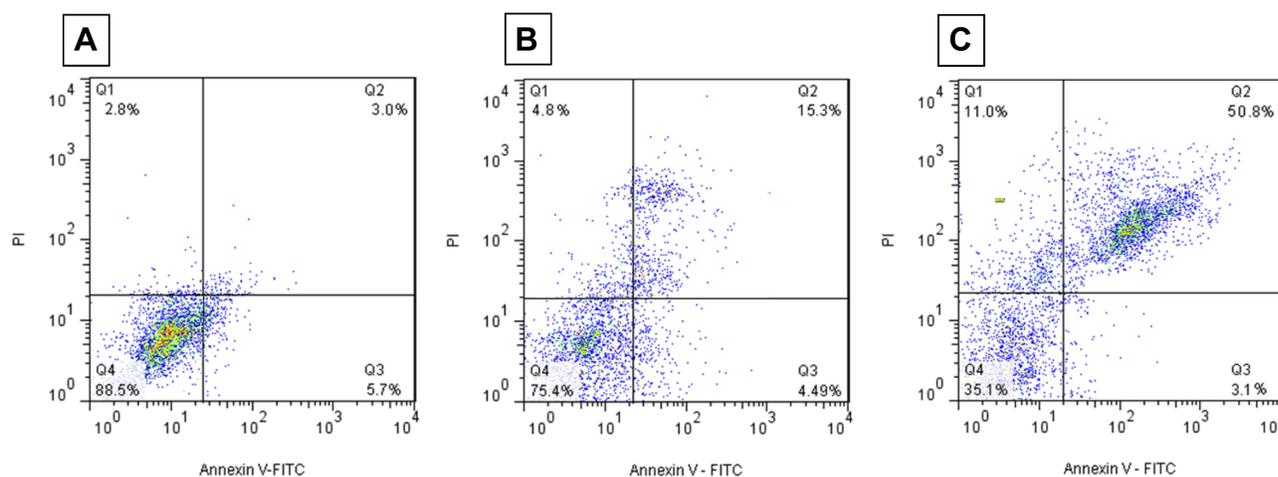
Figure 12 Flow cytometry analysis of α-synuclein aggregates formed with or without ZVFe NPs. SH-SY5Y cells were treated with the negative control group (**A**), α-synuclein fibrils aged for 45 h alone (**B**) or in the presence of ZVFe for 24 h (**C**).

with negative control samples (data not shown). However, the rate of apoptosis (Q2 and Q3, 8.7%) and necrosis (Q4, 2.8%) in control cells increased to 19.79% (**$P<0.01$, different from cells exposed only to control) (Figure 12B), 53.9% (***$P<0.001$, different from cells exposed only to control) (Figure 12C), 4.8% (Fig. 12B), and 11% (**$P<0.01$, different from cells exposed only to control) (Figure 12C) in α-synuclein amyloid- and α-synuclein amyloid/ZVFe NPs-treated samples, respectively. Also, it can be observed that the degree of apoptosis (##$P<0.01$, different from cells exposed only to α-synuclein amyloid) and necrosis (##$P<0.01$, different from cells exposed only to α-synuclein amyloid) in ZVFe NPs/α-synuclein amyloid-treated cells is more severe when compared to the data resulted from the α-synuclein amyloid-treated cells without ZVFe NPs.

Discussion

NPs are almost spontaneously covered with proteins when they reach a biological system, followed by conformational and/or functional changes of the surface-adsorbed state of the protein. Proteins may be adsorbed in a non-destructive or denatured form based on protein compositionand the NP features. The high concentration of bound proteins and the low dimensionality of the NP curvature can increase the possibility of interaction between denatured proteins and subsequent faster fibrillation.[33,34] These features of NPs can affect protein self-assembly mechanisms which may result in distrubtion of crucial biological systems. Increase in disorders due to protein misfolding and fibrillation may also happen after interaction of proteins with NPs. It has been

suggested that interactions with different surfaces could accelerate protein aggregation into amyloid fibrils and increase protein structural alterations associated with other protein misfolding disorders.[35,36]

Several studies show that NPs catalyze protein fibril formation through influencing the structure of the amyloidogenic species formed during fibrillation. For instance, Linse et al., showed that some NPs such as copolymers, cerium, quantum dots, and carbon nanostructures increase the possibility of formation of a censorious site for nucleation of amyloid from human β2-microglobulin.[33] The authors claimed that the determined shorter nucleation process and an increase in the rate of fibrillation are heavily linked to the dose and chemical composition of NPs. As a matter of fact, when proteins are adsorbed on the NP surface, locally enhanced protein doses induce fibril formation. Also, shortened nucleation process may define a mechanism involving NP-derived nucleation, enhancing the risk of destructive and unsafe clusters and fibrillation.[33] Wu et al., also found that Aβ fibril formation occurs in the presence of titanium dioxide (TiO$_2$) NPs with a dose of 10 μg/ml.[36] They revealed that TiO$_2$ NPs could accelerate Aβ fibrillation by shortening the assembly phase as the critical rate-controlling phase of amyloidogenesis.[36] It has also been reported that physico-chemical features of NPs can influence the fibrillation steps of proteins like Aβ 8,.[37–39] In the current study, we observed that ZVFe NPs with a dose of 50 μg/ml could shorten the lag phase of α-synuclein fibrillation and increase the rate of fibrillation. However, it should be noted that there are several studies which indicate that NPs can serve as potential inhibitors of amyloid fibrillation.[40–43] Therefore, it may be

suggested that the physicochemical properties and chemical composition of NPs play pivotal roles in modulating protein aggregation.

Regarding the cytotoxicity effect of NPs alone or in the presence of amyloid fibril, several investigations have also been reported.[44,45] Our cellular results suggest that NPs can show substantial impact on protein conformation which may influence the mortality of host/neighbor cells. Actually, we found that ZVFe NPs binds α-synuclein, promoting protein aggregation and assosiated cytotoxicity.

Indeed, the effects depend on the physicochemical characteristics of protein and NPs.[44] NPs with different physicochemical properties can increase or decrease the fibrillation and corresponding cytotoxicity. For example, Asthana et al., demonstrated that insulin interaction with zinc oxide NPs causes structural rearrangement into amyloid-prone clusters with increased cytotoxic characteristics.[44] Also, Rawat et al., reported that cell membranes can act as modulators of amyloid fibrillation and can target cytotoxicity.[45] In accordance with these reports, we showed that the membrane leakage or necrosis is increased in the presence of α-synuclein amyloid and α-synuclein amyloid/ZVFe NPs. For the cellular assay, some conflicting results have been reported. For example, Liu et al.,[46] Zhang et al.,[47] Yadav et al.,[48] and Malishev et al.,[49] reported that NPs could modulate amyloid-beta fibrillation and relevant cytotoxicity.

The biological system due to the variations in pH and ionic strength can influence on the metal ion release from the NPs and alters the bio-functionality and the side impacts of the NPs-metal ion multiplex.[50] Although, there has been clearly reported adverse impacts from dissolved Fe ions in development of neurodegenerative diseases,[51,52] the ZVFe NPs may exhibit extra adverse effects due to their tendency to agglomeration. It is likely that the ZVFe NPs attach to protein and cell membrane and induce some structural changes and cytotoxicity by transferring electrons to various compounds, causing unwanted interactions.

Therefore, the NPs morphology, composition, diameter, surface charge, and concentration should be optimized in order to moderate the impacts of NPs on proteins and the induced cytotoxicity by protein aggregation. In this regard, the current paper may open new doors for modulating assembly of proteins, detection[53,54] and treating neurodegenerative diseases by novel NPs.

Conclusion

Exploring structural changes of protein incubated with NPs and production of α-synuclein amyloid may provide useful information about treating neurodegenerative diseases. Herein, the effect of ZVFe NPs on the structure and fibrillation of α-synuclein was investigated by different experimental and theoretical studies. Native α-synuclein was demonstrated to aggregate, albeit with a slower rate than in the presence of ZVFe NPs. The presence of ZVFe NPs markedly accelerates the rate of fibrillation phase by shortening the aggregation step and increasing the growth rate. This leads to the production of amyloid fibrils which show more adverse effects against SH-SY5Y cells relative to the data resulted from the absence of the ZVFe NPs. Our data may suggest that bare NPs cannot be used to inhibit the rate of protein fibrillation with unique biotechnological propensities as agents with therapeutic functions. Therefore, NPs should be combined with other potential moieties to induce the necessary molecular forces that control protein nucleation mechanisms.

Acknowledgments

Disclosure

The authors report no conflicts of interest in this work.

References

1. Pomatto LC, Cline M, Woodward N, et al. aging attenuates redox adaptive homeostasis and proteostasis in female mice exposed to traffic-derived nanoparticles ('vehicular smog'). *Free Radical Biol Med*. 2018;1(121):86–97. doi:10.1016/j.freeradbiomed.2018.04.574
2. Wiechers JW, Musee N. Engineered inorganic nanoparticles and cosmetics: facts, issues, knowledge gaps and challenges. *J Biomed Nanotechnol*. 2010;6(5):408–431.
3. Juillerat-Jeanneret L, Dusinska M, Fjellsbø LM, Collins AR, Handy RD, Riediker M. NanoTEST consortium. Biological impact assessment of nanomaterial used in nanomedicine. Introduction to the NanoTEST project. *Nanotoxicology*. 2015;9(sup1):5–12. doi:10.3109/17435390.2013.826743
4. MüLler LK, Simon J, Rosenauer C, MailäNder V, Morsbach S, Landfester K. The transferability from animal models to humans: challenges regarding aggregation and protein corona formation of nanoparticles. *Biomacromolecules*. 2018;19(2):374–385. doi:10.1021/acs.biomac.7b01472
5. Bednarikova Z, Marek J, Demjen E, et al. Effect of nanoparticles coated with different modifications of dextran on lysozyme amyloid aggregation. *J Magn Magn Mater*. 2019;1(473):1–6. doi:10.1016/j.jmmm.2018.10.018
6. Vergara C, Houben S, Suain V, et al. Amyloid-β pathology enhances pathological fibrillary tau seeding induced by Alzheimer PHF in vivo. *Acta Neuropathol*. 2019;10:1–6.
7. Mahmoudi M, Quinlan-Pluck F, Monopoli MP, et al. Influence of the physiochemical properties of superparamagnetic iron oxide NPs on amyloid β protein fibrillation in solution. *ACS Chem Neurosci*. 2013;4(3):475–485. doi:10.1021/cn300196n

8. Mirsadeghi S, Shanehsazzadeh S, Atyabi F, Dinarvand R. Effect of PEGylated superparamagnetic iron oxide nanoparticles (SPIONs) under magnetic field on amyloid beta fibrillation process. *Mater Sci Eng*. 2016;1(59):390–397. doi:10.1016/j.msec.2015.10.026

9. Cabaleiro-Lago C, Quinlan-Pluck F, Lynch I, et al. Inhibition of amyloid β protein fibrillation by polymeric NPs. *J Am Chem Soc*. 2008;130(46):15437–15443. doi:10.1021/ja8041806

10. Gnach A, Lipinski T, Bednarkiewicz A, Rybka J, Capobianco JA. Upconverting nanoparticles: assessing the toxicity. *Chem Soc Rev*. 2015;44(6):1561–1584. doi:10.1039/c4cs00177j

11. Alim MA, Ma QL, Takeda K, et al. xkaji M, Yoshii M, Hisanaga S. Demonstration of a role for α-synuclein as a functional microtubule-associated protein. *J Alzheimer's Dis*. 2004;6(4):435–442.

12. Perez RG, Waymire JC, Lin E, Liu JJ, Guo F, Zigmond MJ. A role for α-synuclein in the regulation of dopamine biosynthesis. *J Neurosci*. 2002;22(8):3090–3099.

13. Clayton DF, George JM. The synucleins: a family of proteins involved in synaptic function, plasticity, neurodegeneration and disease. *Trends Neurosci*. 1998;21(6):249–254.

14. Álvarez YD, Fauerbach JA, Pellegrotti JV, Jovin TM, Jares-Erijman EA, Stefani FD. Influence of gold nanoparticles on the kinetics of α-synuclein aggregation. *Nano Lett*. 2013;13(12):6156–6163. doi:10.1021/nl403490e

15. Yang JA, Johnson BJ, Wu S, Woods WS, George JM, Murphy CJ. Study of wild-type α-synuclein binding and orientation on gold nanoparticles. *Langmuir*. 2013;29(14):4603–4615. doi:10.1021/la400266u

16. Zhu F, Ma S, Liu T, Deng X. Green synthesis of nano zero-valent iron/Cu by green tea to remove hexavalent chromium from groundwater. *J Clean Prod*. 2018;10(174):184–190. doi:10.1016/j.jclepro.2017.10.302

17. Prabu D, Parthiban R, Kumar PS, Namasivayam SK. Synthesis, characterization and antibacterial activity of nano zero-valent iron impregnated cashew nut shell. *Int J Pharm Pharm Sci*. 2015;7:139–141.

18. Stieber M, Putschew A, Jekel M. Treatment of pharmaceuticals and diagnostic agents using zero-valent iron–kinetic studies and assessment of transformation products assay. *Environ Sci Technol*. 2011;45(11):4944–4950. doi:10.1021/es200034j

19. Li H, Zhou Q, Wu Y, Fu J, Wang T, Jiang G. Effects of waterborne nano-iron on medaka (Oryzias latipes): antioxidant enzymatic activity, lipid peroxidation and histopathology. *Ecotoxicol Environ Saf*. 2009;72(3):684–692. doi:10.1016/j.ecoenv.2008.09.027

20. Lee C, Kim JY, Lee WI, Nelson KL, Yoon J, Sedlak DL. Bactericidal effect of zero-valent iron nanoparticles on Escherichia coli. *Environ Sci Technol*. 2008;42(13):4927–4933. doi:10.1021/es800408u

21. Smith MA, Zhu X, Tabaton M, Liu G, et al. Increased iron and free radical generation in preclinical Alzheimer disease and mild cognitive impairment. *J Alzheimer's Dis*. 2010;19(1):363–372. doi:10.3233/JAD-2010-1239

22. González-Lizárraga F, Socías SB, Ávila CL, et al. Repurposing doxycycline for synucleinopathies: remodelling of α-synuclein oligomers towards non-toxic parallel beta-sheet structured species. *Sci Rep*. 2017;3(7):41755. doi:10.1038/srep41755

23. Mahdavimehr M, Meratan AA, Ghobeh M, Ghasemi A, Saboury AA, Nemat-Gorgani M. Inhibition of HEWL fibril formation by taxifolin: mechanism of action. *PLoS One*. 2017;12(11):e0187841. doi:10.1371/journal.pone.0187841

24. Aghili Z, Taheri S, Zeinabad HA, et al. Investigating the interaction of Fe nanoparticles with lysozyme by biophysical and molecular docking studies. *PLoS One*. 2016;11(10):e0164878. doi:10.1371/journal.pone.0164878

25. Ritchie DW, Venkatraman V. Ultra-fast FFT protein docking on graphics processors. *Bioinformatics*. 2010;26(19):2398–2405. doi:10.1093/bioinformatics/btq444

26. Rappé AK, Casewit CJ, Colwell KS, Goddard III WA, Skiff WM. UFF, a full periodic table force field for molecular mechanics and molecular dynamics simulations. *J Am Chem Soc*. 1992;114(25):10024–10035. doi:10.1021/ja00051a040

27. Sedaghat Anbouhi T, Mokhtari Esfidvajani E, Nemati F, et al. Albumin binding, anticancer and antibacterial properties of synthesized zero valent iron nanoparticles. *Int J Nanomedicine*. 2018;2019(14):243–256.

28. Asl BA, Mogharizadeh L, Khomjani N, et al. Probing the interaction of zero valent iron nanoparticles with blood system by biophysical, docking, cellular, and molecular studies. *Int J Biol Macromol*. 2018;1(109):639–650. doi:10.1016/j.ijbiomac.2017.12.085

29. Chen SW, Drakulic S, Deas E, et al. Structural characterization of toxic oligomers that are kinetically trapped during α-synuclein fibril formation. *Proc National Acad Sci*. 2015;8:201421204.

30. Galvagnion C, Buell AK, Meisl G, et al. Lipid vesicles trigger α-synuclein aggregation by stimulating primary nucleation. *Nat Chem Biol*. 2015;11(3):229. doi:10.1038/nchembio.1750

31. Lee JE, Sang JC, Rodrigues M, et al. Mapping surface hydrophobicity of α-synuclein oligomers at the nanoscale. *Nano Lett*. 2018;18(12):7494–7501. doi:10.1021/acs.nanolett.8b02916

32. Hanwell MD, Curtis DE, Lonie DC, Vandermeersch T, Zurek E, Hutchison GR. Avogadro: an advanced semantic chemical editor, visualization, and analysis platform. *J Cheminform*. 2012;4(1):17. doi:10.1186/1758-2946-4-17

33. Linse S, Cabaleiro-Lago C, Xue WF, et al. Nucleation of protein fibrillation by nanoparticles. *Proc National Acad Sci*. 2007;104(21):8691–8696. doi:10.1073/pnas.0701250104

34. Lynch I, Dawson KA. Protein-nanoparticle interactions. *Nano Today*. 2008;3(1–2):40–47. doi:10.1016/S1748-0132(08)70014-8

35. Wang W, Nema S, Teagarden D. Protein aggregation—pathways and influencing factors. *Int J Pharm*. 2010;390(2):89–99. doi:10.1016/j.ijpharm.2010.02.025

36. Wu WH, Sun X, Yu YP, et al. TiO 2 nanoparticles promote β-amyloid fibrillation in vitro. *Biochem Biophys Res Commun*. 2008;373(2):315–318. doi:10.1016/j.bbrc.2008.06.035

37. Cabaleiro-Lago C, Szczepankiewicz O, Linse S. The effect of nanoparticles on amyloid aggregation depends on the protein stability and intrinsic aggregation rate. *Langmuir*. 2012;28(3):1852–1857. doi:10.1021/la203078w

38. Kim Y, Park JH, Lee H, Nam JM. How do the size, charge and shape of nanoparticles affect amyloid β aggregation on brain lipid bilayer? *Sci Rep*. 2016;19(6):19548. doi:10.1038/srep19548

39. Álvarez YD, Pellegrotti JV, Stefani FD. Gold nanoparticles as nucleation centers for amyloid fibrillation. In: Santamaria F, Peralta XG, editors. *Use of Nanoparticles in Neuroscience*. New York, NY: Humana Press; 2018:269–291.

40. Mandal S, Debnath K, Jana NR, Jana NR. Trehalose-functionalized gold nanoparticle for inhibiting intracellular protein aggregation. *Langmuir*. 2017;33(49):13996–14003. doi:10.1021/acs.langmuir.7b02202

41. Moore KA, Pate KM, Soto-Ortega DD, et al. Influence of gold nanoparticle surface chemistry and diameter upon Alzheimer's disease amyloid-β protein aggregation. *J Biol Eng*. 2017;11(1):5. doi:10.1186/s13036-017-0047-6

42. Pradhan N, Jana NR, Jana NR. Inhibition of protein aggregation by iron oxide nanoparticles conjugated with glutamine-and proline-based osmolytes. *ACS Appl Nano Mater*. 2018;1(3):1094–1103. doi:10.1021/acsanm.7b00245

43. Pradhan N, Debnath K, Mandal S, Jana NR, Jana NR. Antiamyloidogenic chemical/biochemical-based designed nanoparticle as artificial chaperone for efficient inhibition of protein aggregation. *Biomacromolecules*. 2018;19(6):1721–1731. doi:10.1021/acs.biomac.8b00671

44. Asthana S, Hazarika Z, Nayak PS, et al. Insulin adsorption onto zinc oxide nanoparticle mediates conformational rearrangement into amyloid-prone structure with enhanced cytotoxic propensity. *Biochimica Et Biophys Acta (Bba)-Gen Subj*. 2019;1863 (1):153–166. doi:10.1016/j.bbagen.2018.10.004

45. Rawat A, Langen R, Varkey J. Membranes as modulators of amyloid protein misfolding and target of toxicity. *Biochimica Et Biophys Acta (Bba)-Biomembr*. 2018;1860:1863–1875. doi:10.1016/j.bbamem.2018.04.011

46. Liu G, Men P, Kudo W, Perry G, Smith MA. Nanoparticle–chelator conjugates as inhibitors of amyloid-β aggregation and neurotoxicity: a novel therapeutic approach for Alzheimer disease. *Neurosci Lett*. 2009;455(3):187–190. doi:10.1016/j.neulet.2009.03.064

47. Zhang J, Zhou X, Yu Q, et al. Epigallocatechin-3-gallate (EGCG)-stabilized selenium nanoparticles coated with Tet-1 peptide to reduce amyloid-β aggregation and cytotoxicity. *ACS Appl Mater Interfaces*. 2014;6(11):8475–8487. doi:10.1021/am501341u

48. Yadav KK, Arakha M, Das B, Mallick B, Jha S. Preferential binding to zinc oxide nanoparticle interface inhibits lysozyme fibrillation and cytotoxicity. *Int J Biol Macromol*. 2018;1(116):955–965. doi:10.1016/j.ijbiomac.2018.05.098

49. Malishev R, Arad E, Bhunia SK, et al. Chiral modulation of amyloid beta fibrillation and cytotoxicity by enantiomeric carbon dots. *Chem Commun*. 2018;54(56):7762–7765. doi:10.1039/c8cc03235a

50. Hahn A, Fuhlrott J, Loos A, Barcikowski S. Cytotoxicity and ion release of alloy nanoparticles. *J Nanopart Res*. 2012;14(1):686. doi:10.1007/s11051-011-0686-3

51. Guo C, Liu JL, Fan YG, Yang ZS, Wang ZY. Iron and Alzheimer's disease: from pathogenesis to therapeutic implications. *Front Neurosci*. 2018;12:632. doi:10.3389/fnins.2018.00044

52. Wojtunik-Kulesza K, Oniszczuk A, Waksmundzka-Hajnos M. An attempt to elucidate the role of iron and zinc ions in development of Alzheimer's and Parkinson's diseases. *Biomed Pharmacother*. 2019;1(111):1277–1289. doi:10.1016/j.biopha.2018.12.140

53. Xia N, Zhou B, Huang N, Jiang M, Zhang J, Liu L. Visual and fluorescent assays for selective detection of beta-amyloid oligomers based on the inner filter effect of gold nanoparticles on the fluorescence of CdTe quantum dots. *Biosens Bioelectron*. 2016;15 (85):625–632. doi:10.1016/j.bios.2016.05.066

54. Xia N, Wang X, Zhou B, Wu Y, Mao W, Liu L. Electrochemical detection of amyloid-β oligomers based on the signal amplification of a network of silver nanoparticles. *ACS Appl Mater Interfaces*. 2016;8 (30):19303–19311. doi:10.1021/acsami.6b05423